A common single nucleotide polymorphism impairs B-cell activating factor receptor's multimerization, contributing to common variable immunodeficiency

Kathrin Pieper, PhD[a,b], Marta Rizzi, MD, PhD[a]*, Matthaios Speletas, MD, PhD[c]*, Cristian R. Smulski, PhD[d]*, Heiko Sic, PhD[a,b], Helene Kraus, MSc[a,b], Ulrich Salzer, MD[a], Gina J. Fiala, MSc[a,e], Wolfgang W. Schamel, PhD[a,e], Vassilios Lougaris, MD[f], Alessandro Plebani, MD[f], Lennart Hammarstrom, MD, PhD[g], Mike Recher, MD[h], Anastasios E. Germenis, MD, PhD[c], Bodo Grimbacher, MD[a], Klaus Warnatz, MD, PhD[a], Antonius G. Rolink, PhD[i], Pascal Schneider, PhD[d], Luigi D. Notarangelo, MD[i], Hermann Eibel, PhD[a]

a: the Centre for Chronic Immunodeficiency, University Medical Centre Freiburg, Freiburg, Germany
b: the Faculty of Biology, Albert-Ludwigs-University, Freiburg, Germany
c: the Faculty of Medicine, Department of Immunology & Histocompatibility, University of Thessaly, Larissa, Greece
d: the Faculty of Medicine, Department of Biochemistry, University of Lausanne, Lausanne, Switzerland
e: the Faculty of Biology, Institute of Biology III, and BIOSS Center for Biological Signalling Studies, Albert-Ludwigs University Freiburg, Freiburg, Germany
f: the Pediatric Clinic and A. Nocivelli Institute of Molecular Medicine, University of Brescia, Spedali Civili, Brescia, Italy
g: the Department of Laboratory Medicine, Karolinska Institutet, Huddinge, Sweden
h: the Division of Immunology and The Manton Center for Orphan Disease Research Center, Children's Hospital, Boston, Mass
i: Developmental and Molecular Immunology, Department of Biomedicine, University of Basel, Basel, Switzerland.

*These authors contributed equally to this work.

E-mail: hermann.eibel@uniklinik-freiburg.de.

Letter to the Editor

Binding of the B-cell activating factor (BAFF) to its receptor (BAFFR) is essential for B-cell development and survival.[1] A homozygous deletion in the BAFFR-encoding TNFRSF13C gene causes common variable immunodeficiency (CVID),[2] one of the most frequent primary antibody deficiencies in humans characterized by the strong reduction in immunoglobulin serum titers.[3] Five single-nucleotide polymorphisms resulting in BAFFR missense mutations have been found. Interestingly, in patients with CVID, the single-nucleotide polymorphism Pro21>Arg (P21R) (c.62C>G; rs77874543) has been described but its effects on BAFFR function and disease association are unknown.[4]

On comparing BAFFR expression by and BAFF binding to B cells, we observed that B lymphocytes expressing the BAFFR P21R mutation bound less BAFF than did cells expressing only major (wild-type [WT]) alleles (Fig 1, A) although BAFFR expression levels were very similar (Fig 1, B). Binding studies with B cells from healthy donors (Fig E1) and from patients with CVID (Fig E2) revealed reduced BAFF binding by cells expressing homozygous or heterozygous P21R BAFFR under ligand saturation, showing that the heterozygous P21R allele dominantly interferes with BAFF binding.

BAFFR is an atypical member of the tumor necrosis factor receptor (TNFR) family. It carries only a single, truncated, cysteine-rich domain (CRD) in its extracellular region. Typical TNFR family members including CD40, TNFR1, Fas, TRAILR4, and the BAFF-binding receptor TACI, which is related to BAFFR, assemble into homo-oligomers in the absence of ligand.[5,6] TNFR clustering is a prerequisite for ligand binding and is catalyzed by intramolecular interactions between the preligand assembly domains (PLADs). PLADs are located in the N-terminal CRD and do not overlap with the ligand-binding domain.[5] P21 points away from BAFF in the BAFF/BAFFR complex (Fig E3). Superimposing the structural model of BAFFR on the CRD1 of TNFR1 shows that P21 corresponds to Q46 of TNFR1 (Fig E3, B), a residue involved in TNFR1-TNFR1 interactions in the crystal structure of dimeric TNFR1 (Fig E3, C). Therefore, we speculated that the P21 residue might form part of the yet to be identified PLAD of BAFFR and tested whether BAFFR WT or BAFFR P21R chains self-associate like other TNFR family members. On combining blue-native-PAGE/1-dimensional and SDS-PAGE/2-dimensional, we found that BAFFR WT formed high molecular weight (MW) complexes up to 1000 kDa in size in EBV lines (Fig 1, C) and primary B cells (Fig E4A). In contrast, BAFFR P21R formed only a few high MW complexes, suggesting that the heterozygous and homozygous P21R BAFFR mutation disturbs ligand-independent BAFFR multimerization. To prove that 2-dimensional gel electrophoresis is a suitable method to detect complex formation, we compared PLAD-containing and PLAD-deleted Fas by using blue-native/SDS

PAGE. Like BAFFR P21R, truncated Fas failed to form high MW complexes (Fig E4, B) in spite of similar cell surface expression (Fig E4, C).
In an independent approach, we determined BAFFR multimerization by fluorescence resonance energy transfer (FRET) of full-length WT or P21R BAFFR fused to eYFP or eCFP. Again, interactions between Fas polypeptide chains served as control for complex formation. Similar to Fas, cells expressing the BAFFR/BAFFR combination revealed strong FRET signals confirming that BAFFR, like Fas, can self-associate (Fig E5). Compared with BAFFR WT/WT combination, we detected significantly less FRET-positive cells for BAFF-R WT/P21R and P21R/P21R, mimicking hetero- and homozygous conditions. Combinations of Fas/BAFFR or BAFFR/Fas produced only background signals.
Therefore, we propose that BAFFR contains a PLAD that includes residue P21, which facilitates BAFFR preassembly into clusters and therefore BAFF binding. This implies that in contrast to other TNFR family members,5 the single CRD of BAFFR carries in addition to the ligand-binding domain a PLAD.
Deletion of BAFFR in humans blocks B-cell development at the stage of transitional B cells.2 However, we did not find changes in numbers or in B-cell subsets in individuals expressing BAFFR P21R compared with WT (see Fig E6 A). Notably, individuals heterozygous for the BAFFR deletion2 express only approximately 50% of WT BAFFR levels but have normal B-cell numbers and B-cell subsets (Fig E6 B and C). Thus, a 50% reduction in BAFF binding to BAFFR per se as observed in BAFFR P21R-expressing B cells does not suffice to affect B-cell survival and subset composition.
BAFF binding to BAFFR activates NF-kB2. Thus, we analyzed whether changes in BAFFR clustering impair NF-kB2 processing. Addition of BAFF to BAFFR WT-expressing cells induced processing of NF-kB2 p100 into p52 (Fig E7 A), but in P21R-expressing cells, the ratio of p52/p100 was always lower (Fig E7, B). Therefore, by disturbing BAFFR clustering, the P21R mutation impairs BAFF-induced NF-kB2 activation.
BAFF acts as an essential prosurvival factor not only for resting B cells but also for activated B cells in T-independent immune responses.[7] To determine whether the P21R mutation disturbs B cell activation, we stimulated B lymphocytes from healthy individuals expressing BAFFR WT or BAFFR P21R in vitro with CpG DNA and anti-IgM and compared B-cell numbers (Fig 1, D) and IgM secretion (Fig 1, E). In contrast to BAFFR WT cells, addition of BAFF neither increased cell numbers nor enhanced IgM secretion of activated BAFFR P21R-expressing B lymphocytes. In accordance with binding and FRET studies, in vitro responses of B cells with heterozygous BAFFR P21R alleles from healthy donors (Fig E8 A) and patients with CVID (Fig E8 B) were reduced. However, the more severe decrease in cell numbers of CVID B cells might mirror additional B-cell defects. Differences found after CpG DNA and anti-IgM stimulation were not caused by intrinsic defects because P21R B lymphocytes responded equally well to the activation with CD40 ligand and IL21-Fc (Fig E9).
Patients suffering from CVID frequently fail to induce T-independent immune responses and have recurrent bacterial respiratory infections,[3] suggesting that the P21R-encoding TNFRSF13C allele might be a risk factor for CVID. Analyzing the P21R frequency in 1572 healthy controls and 324 patients with CVID by RFLP and sequence analysis revealed an allele frequency of 10.2%for P21R in patients with CVID and of 6.7%in controls corresponding to an odds ratio of 1.57 (P5.0026; Table I). In contrast to the CVID-causing homozygous deletion of the BAFFR gene, the P21R allele is also found in healthy individuals. Thus, disturbed BAFFR complex formation is not severe enough to result in CVID but has to combine with other risk factors to cause the clinical symptoms of CVID. It is of interest that heterozygous TACI mutations were also described as risk factors increasing the susceptibility to CVID.[6] Therefore, missense mutations in 2 receptors that bind BAFF as a common ligand and that are critical for B-cell development and responses are found at surprisingly high frequencies in the healthy population.
In conclusion, our work provides mechanistic insights how impaired preassembly of BAFFR caused by homo- or heterozygous P21R BAFFR mutation may contribute to the development of CVID. In combination with other risk alleles, BAFFR, like TACI, seem to represent one component of multigenic defects that result in primary antibody deficiency.

Acknowledgment
We thank Beate Fischer, Kerstina Melkaoui (CCI, Freiburg), Evangelia Karamouti (University of Thessaly), and Laure Willen (University of Lausanne) for their technical assistance. We are grateful to Hans-Hartmut Peter, Andreas H. Kottmann, and Jean-ClaudeWeill for their suggestions and comments and for critically reading the manuscript.
This work was supported by the German Cancer Research Fund (grant no. 108935 to H.E. and K.P.), the European Union 7th framework grant (no. HEALTH-F2-2008-201549 to H.E., B.G., U.S., L.H., V.L., and A.P.), the Federal Ministry of Education and Research (grant no. BMBF 01 E0 08 03 to M. Rizzi), the Swiss National Science Foundation (grant no. PASMP3-127678/1 to M. Recher and grant no. 31003A_138065 to P.S.), Merck-Serono (to P.S.), and the Deutsche-Forschungsgemeinschaft (grant no. TRR130 TP06 to H.E., grant no. EXC294 to W.W.S., and SFB620 project C7 to U.S.).

Disclosure of potential conflict of interest

M. Speletas is employed by the University of Thessaly; has received research support from General Secretariat of Research; has received lecture fees from Amgen Hellas for immunology lectures; and has received travel fees from Shire Hellas, Behring Hellas, and Bristol-Meyer Hellas.

L. Hammarstrom has received research support from the Swedish Research Council.

M. Recher has received research support from the Swiss National Science Foundation and the University of Basel, Switzerland.

A. E. Germenis has received consultant fees from Novartis and Shire, is employed by the University of Thessaly, has received lecture fees from Amgen and Novartis, and has received travel fees from Shire.

B. Grimbacher has received research support from University College London (UCL) (FP7 Eu Grant [EURO-PADnet Health-F2-2008-201549]) and Uniklinik Freiburg (BMBF 01 Eo0803); is employed by UCL; receives royalties from Springer; and has received travel fees from CSL Behring, the American Academy of Allergy, Asthma & Immunology, Japanese Society of Immunodeficiency, European Society of Immunodeficiency, Latin American Society of Immunodeficiency, Primary Immunodeficiency Meeting.

K. Warnatz has received research support and travel support from EURPADnet EU-FP7; has received lecture fees and honoraria from Baxter, GlaxoSmithKline, CSL Behring, Pfizer, the American Academy of Allergy, Asthma & Immunology, Biotest, and Novartis Pharma; is employed by a CCI grant from Bundesministerium für Bildung und Forschung; has research support pending from Deutsche Forschungsgesellschaft; and has received fees for manuscript preparation from UCB Pharma.

P. Schneider has received research support from Merck-Serono and Edimer Pharmaceuticals and receives royalties from Adipogen.

L. D. Notarangelo is a board member for a program in Molecular and Cellular Medicine, the Pediatric University Hospital ‘‘meyer,’’ and the Board of Scientific Counselors, the National Institues of Allergy and Infectious Diseases, and the National Institutes of Health (NIH); is employed by Boston Children’s Hospital; has received research support from the NIH and March of Dimes; and receives royalties from UpToDate.

H. Eibel has received research support from the German Cancer Research Fund and Deutsche Forschungsgemeinschaft.

The rest of the authors declare that they have no relevant conflicts of interest.

References

1. Sasaki Y, Casola S, Kutok JL, Rajewsky K, Schmidt-Supprian M. TNF family member B cell-activating factor (BAFF) receptor-dependent and -independent roles for BAFF in B cell physiology. J Immunol 2004;173:2245-52.

2. Warnatz K, Salzer U, Rizzi M, Fischer B, Gutenberger S, Bohm J, et al. B-cell activating factor receptor deficiency is associated with an adult-onset antibody deficiency syndrome in humans. Proc Natl Acad Sci U S A 2009;106:13945-50.

3. Notarangelo LD. Primary immunodeficiencies. J Allergy Clin Immunol 2010;125: S182-94.

4. Losi CG, Silini A, Fiorini C, Soresina A, Meini A, Ferrari S, et al. Mutational analysis of human BAFF receptor TNFRSF13C (BAFF-R) in patients with common variable immunodeficiency. J Clin Immunol 2005;25:496-502.

5. Chan FK. Three is better than one: pre-ligand receptor assembly in the regulation of TNF receptor signaling. Cytokine 2007;37:101-7.

6. Garibyan L, Lobito AA, Siegel RM, Call ME, Wucherpfennig KW, Geha RS. Dominant-negative effect of the heterozygous C104R TACI mutation in common variable immunodeficiency (CVID). J Clin Invest 2007;117:1550-7.

7. Cerutti A, Cols M, Puga I. Marginal zone B cells: virtues of innate-like antibody producing lymphocytes. Nat Rev Immunol 2013;13:118-32.

Table I. BAFFR P21R frequencies in patients with CVID and controls

	Individuals					Allele frequency (%)			
Cohort	WT	HET P21R	HOM P21R	P21R alleles (n)	WT alleles (n)	P21R	WT	P value	Odds ratio
HDs	1375	183	14	211	2933	6.7	93.3		
CVID	262	58	4	66	582	10.2	98.8	0.0026	1.57

The table shows the numbers and the allele frequencies of BAFFR WT, homozygous (HOM), and heterozygous (HET) P21R mutations in healthy donors (HDs) and patients with CVID. P value and odds ratio were calculated by using a 2-tailed Fisher exact test within 95% CIs.

Figures

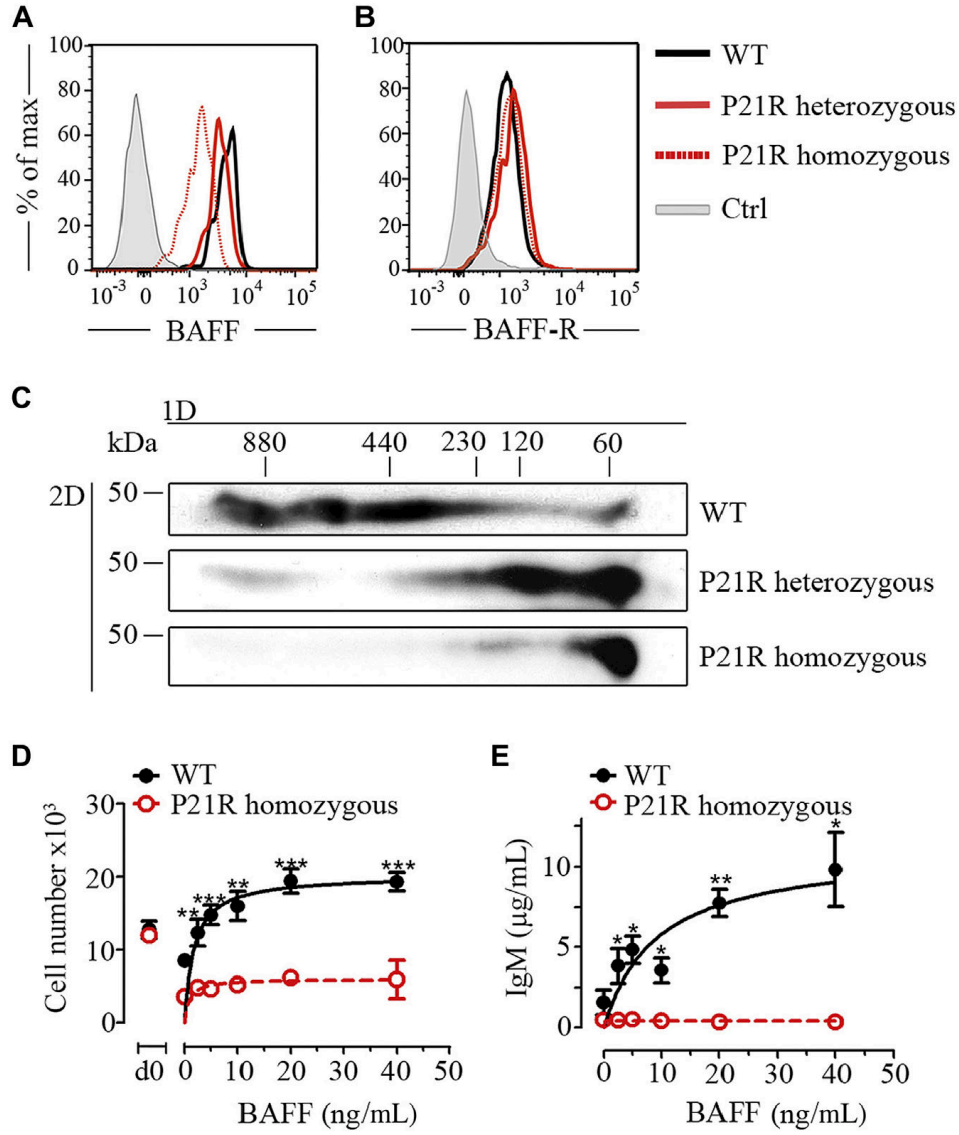

Figure 1. BAFF binding to (A) and BAFFR expression (B) by B cells from healthy donors. C, BAFFR immunoblots of 2-dimensional gel electrophoresis performed with EBV cell lines (n > 3). Cell numbers (D) and IgM secretion (E) of primary B cells activated with CpG DNA, anti-IgM, and BAFF. Fig 1, D and E show mean ± SD of triplicates. *P < 0.05; **P < 0.01; and ***P < 0.001.

Extended data

Methods

Patients and healthy donors

Samples were collected in Freiburg, Brescia, and Larissa and at the Karolinska Institute after informed written consent in full accordance with the declaration of Helsinki. All local ethical commissions including the ethics committee of the Albert-Ludwigs-University Freiburg (approval 78/2001) approved the analyses. Patients and controls were aged between 17 and 75 years.

B-cell activation

Magnetic cell sorting–sorted (Miltenyi Biotec, Bergisch Gladbach, Germany) $CD19^+$ human B cells were stimulated with 2 mg/mL $F(ab')_2$ goat anti-human IgM (Southern Biotech, Birmingham, Ala), 0.5 nmol/mL CpG DNA (Apara Biosciences), and human BAFF hexamers produced in HEK293T cells transduced with a BAFF expression vector encoding the signal peptide and trimerization domain of human adiponectin (aa1-114) fused to the extracellular part of human BAFF (aa134-285). The production of the CD40 ligand and IL21-Fc has been described previously.[E1] The absolute cell number was determined at the beginning of the experiment (d0) and after 6 days by counting the events by flow cytometry in the $CD19^+$ 4'-6-diamidino-2-phenylindole $(DAPI)^-$ gate.

Flow cytometry

Cells were stained with fluorochrome-conjugated antibodies anti-IgM-Cy5 (Jackson Immunoresearch), anti-CD27-PerCP-Cy5.5 (Biolegend, San Diego, Calif), anti-CD38-Pe-Cy7, and anti-CD19-APC-H7 (Becton Dickinson, BD, Franklin Lakes, NJ). Human BAFFR was stained with biotinylated mAb huBR9 produced by one of us (A.G.R.) and streptavidin-APC (BD). Samples were acquired on a FACS Canto II (BD) and analyzed with FlowJo software (Tree Star Inc, Ashland, Ore). DAPI was used to exclude dead cells.

BAFF binding

BAFF binding was analyzed by flow cytometry using equal numbers of $CD19^+DAPI^-$ primary B cells co-stained with different amounts of recombinant human FLAG-tagged BAFF (Enzo Life Sciences, Framingdale, NY) and APC-conjugated anti-FLAG mAb M2 (Sigma-Aldrich, Deisenhofen, Germany).

Two-dimensional gel electrophoresis

Blue-native-PAGE was performed with Triton X-100 containing lysis buffer as described[E2] following SDS-PAGE separation. Proteins were detected by immunoblotting by using rabbit antihuman BAFFR (Sigma-Aldrich).

FRET

HEK293T cells were transfected transiently with expression vectors encoding full-length BAFFR C-terminally fused to eYFP or eCFP. FRET signals of more than 1000 double-positive cells were recorded 16 hours posttransfection by using a LSRII (BD Biosciences) flow cytometer with 488, 405 nm lasers and 530/30, 450/50 filters. An eCFP-eYFP fusion protein served as positive control and cotransfection of eCFP and eYFP as negative control according to Banning et al.[E3]

Plasmids

MIGR1-based retroviral vectors for WT BAFFR and the deletion mutant have been described previously.[E1] The P21R mutation was introduced into MIGR-BAFFR-IRES-GFP by in vitro mutagenesis using the oligonucleotide (Apara Biosciences) 5'-gacccccacg ccctgcgtcc gggccgagt gcttcgacct cg-3'. Plasmids were used for retroviral transduction of ST2 cells.

NF-kB2 processing

ST2 cells expressing BAFFR were incubated with BAFF for 16 hours. Cellular lysates were analyzed by immunoblotting using an anti-NF-lB p52 mAb (Millipore, Darmstadt, Germany).

Mutation analysis

Exon 1 of the TNFRSF13C gene was amplified from genomic DNA by PCR by using the primers 5'-agcctcagtccccgcagct-3' and 5'-cggcagctgcggggagaac- 3' (Apara Biosciences). The 223bp PCR product was digested by EagI (New England Biolabs, Ipswich, Mass).

Statistical analysis

Statistical analysis was performed using unpaired, 2-tailed student t test, and P values of less than 0.05 were considered to be statistically significant. Analysis of allele frequency was done by using chi-square and Fisher exact test with GraphPad Prism software (GraphPad Software, La Jolla, Calif).

References

E1. Warnatz K, Salzer U, Rizzi M, Fischer B, Gutenberger S, Bohm J, et al. B-cell activating factor receptor deficiency is associated with an adult-onset antibody deficiency syndrome in humans. Proc Natl Acad Sci U S A 2009;106:13945-50.

E2. Swamy M, Siegers GM, Minguet S, Wollscheid B, Schamel WW. Blue native polyacrylamide gel electrophoresis (BN-PAGE) for the identification and analysis of multiprotein complexes. Sci STKE 2006;2006:pl4.

E3. Banning C, Votteler J, Hoffmann D, Koppensteiner H, Warmer M, Reimer R, et al. A flow cytometry-based FRET assay to identify and analyse protein-protein interactions in living cells. PLoS One 2010;5:e9344.

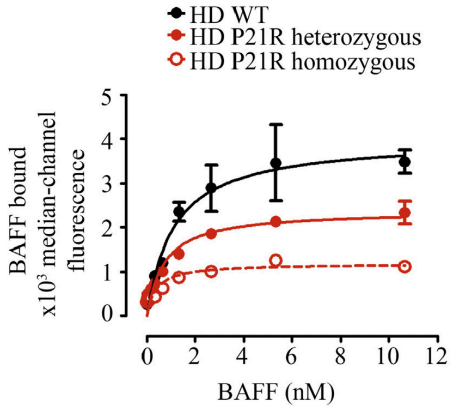

Figure E1: Dose-dependent BAFF binding to primary B cells from healthy donors with heterozygous or homozygous P21R BAFFR mutations or WT BAFFR.

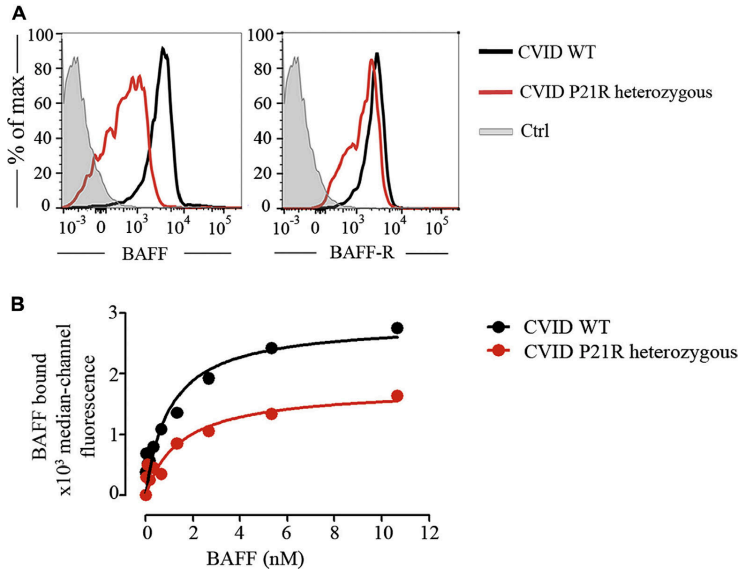

Figure E2. BAFF binding (A), BAFFR expression (B), and dose-dependent BAFF binding plots of primary B cells
isolated from patients with CVID with either WT BAFFR or a heterozygous P21R BAFFR mutation.

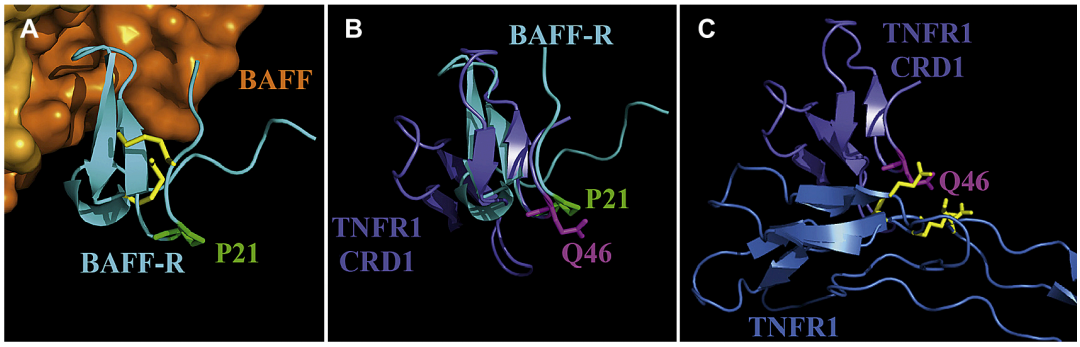

Figure E3. A, Structural modeling of BAFF (orange) bound to BAFFR (cyan); green: P21. B, Superimposition of BAFFR (cyan) and CRD1 of TNFR1 (violet); green: P21 of BAFFR; magenta: Q46 of TNFR1. C, Portion of TNFR1 dimer (violet and blue). Residues close to Q46 shown in yellow. Figures were drawn with PyMol by using the pdb files 1OQE and 1NCF.

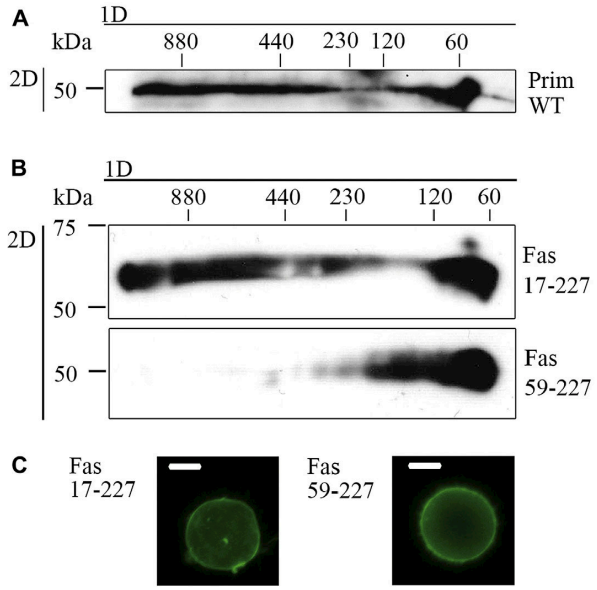

Figure E4. A, BAFFR-specific immunoblots of 2D gel electrophoresis (1-dimensional, BN-PAGE; 2D, SDS-PAGE) with primary B cells. B, 2D-PAGE of HEK293T cells expressing PLAD-containing (Fas17-227) or PLAD-deleted Fas (Fas59-227). Fas was detected by immunoblotting. C, Fluorescence microscopy of Fas17-227 and Fas59-227 YFP fusion proteins expressed in HEK293T cells; scale bar 10 µm. BN, Blue-native; 1D, first dimension; 2D, second dimension.

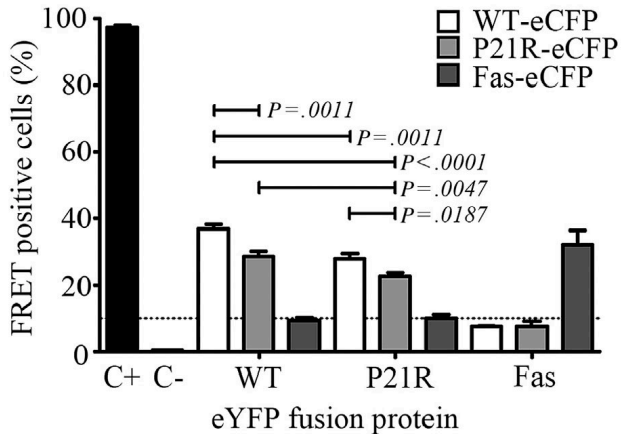

Figure E5. Decreased FRET in P21R-coexpressing cells. BAFFR WT, P21R, and Fas were C-terminally fused to eYFP and eCFP. Percentage of FRET-positive cells was recorded by flow cytometry of coexpressing HEK293T cells. C+, eCFP-eYFP fusion proteins; C-, separate expression of eCFP and eYFP. Results shown are means ± SD of 8 independent experiments. The dotted line indicates background.

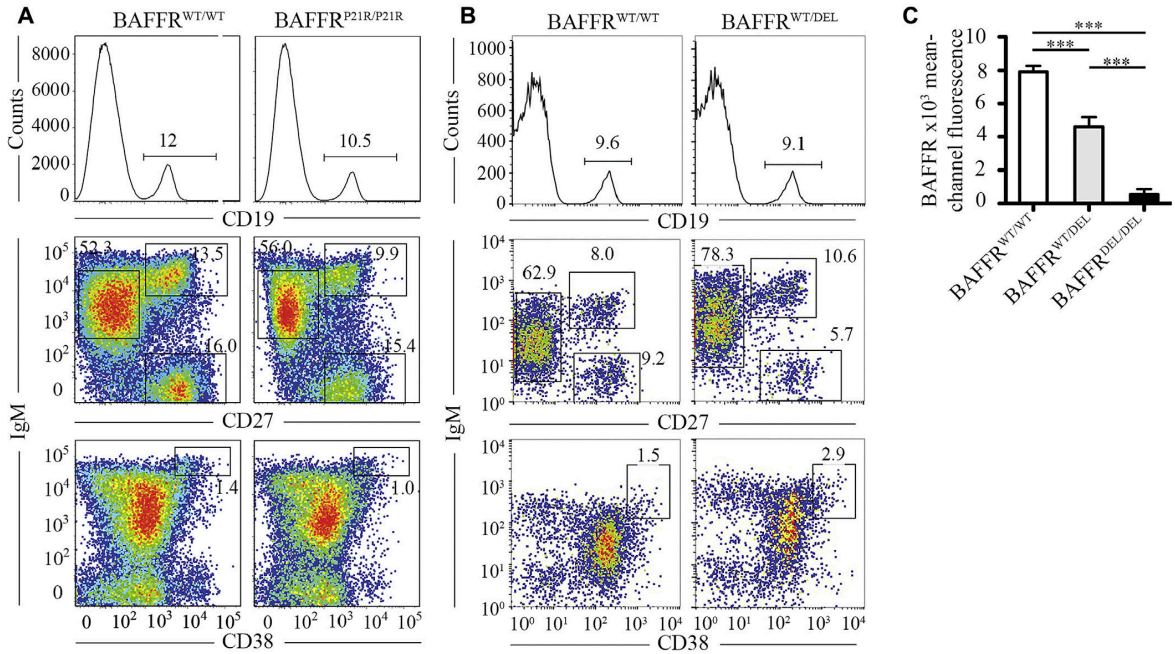

Figure E6. B-cell subsets of individuals with BAFFR WT (BAFFR$^{WT/WT}$), homozygous P21R (BAFFR$^{P21R/P21R}$). (A), or heterozygous BAFFR deletion mutation (BAFFR$^{WT/DEL}$) (B). Histograms show percentages of B cells in PBMCs. FACS plots display CD19^{+} B cells and percentages of CD19^{+}IgM^{+}CD38^{high} transitional, CD19^{+}IgM^{+}CD27^{-} follicular, CD19^{+}IgM^{high}CD27^{+} MZ, and CD19^{+}IgM^{-} CD27^{+} switched-memory B cells. C, BAFFR expression on CD19^{+} B cells; ***P < 0.001. FACS, Fluorescence-activated cell sorting.

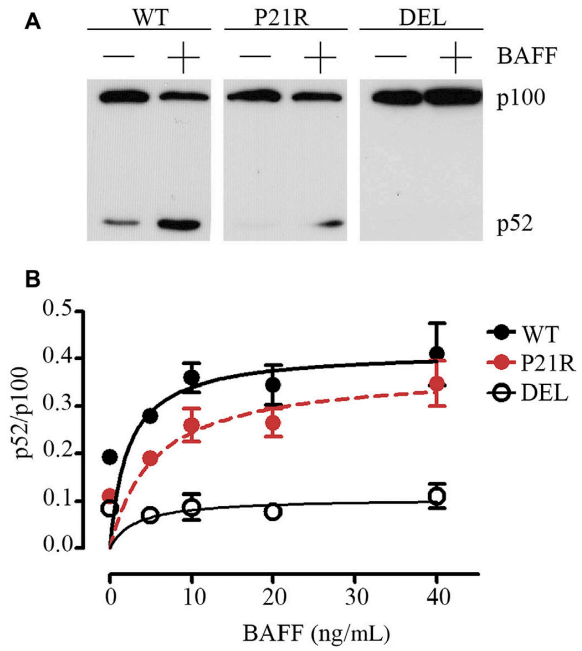

Figure E7. A, Immunoblot analysis of NF-kB2 processing in BAFFR transduced ST2 cells cultivated with (+) or without (-) BAFF. B, Concentration-dependent p52/p100 NF-kB2 ratio. Mean ± SD of 4 independent experiments.

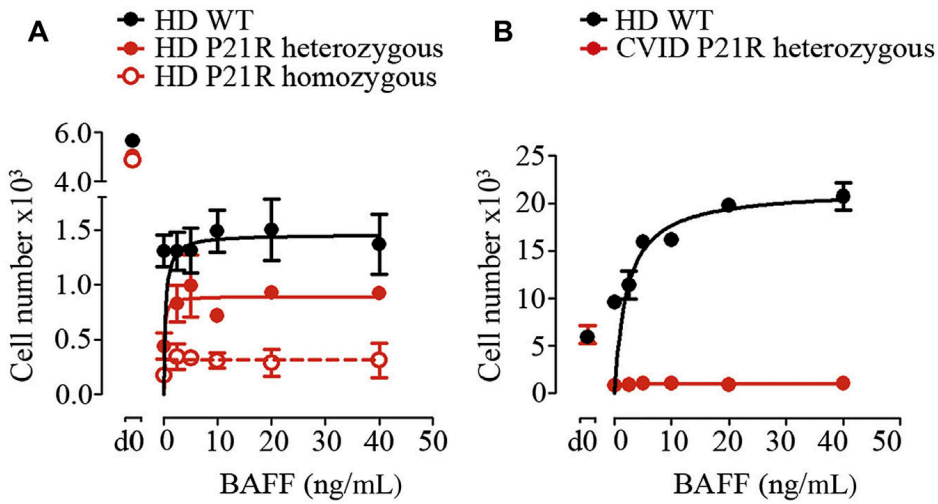

Figure E8. Primary B cells from a healthy donor (A) and a patient with CVID (B) were activated in vitro with CpG DNA, anti-IgM, and BAFF as indicated. Cell numbers were analyzed in the beginning (d0) and after 6 days of cultivation. Plots show mean ± SD of triplicates.

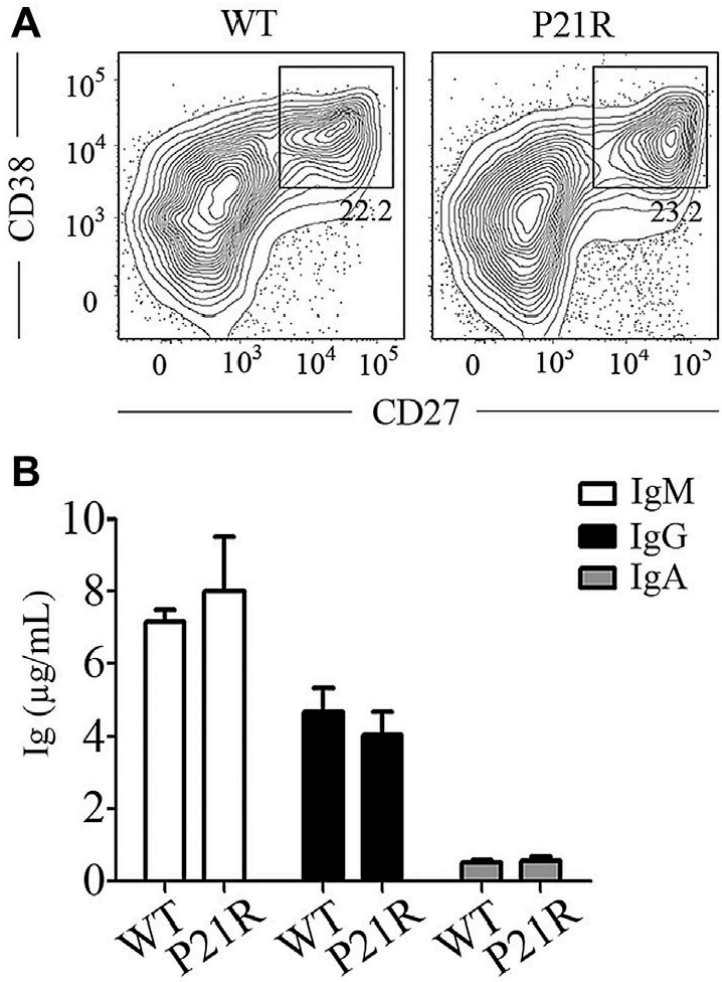

Figure E9. $CD19^+$ human B cells expressing BAFFR WT or homozygous P21R were cultivated in vitro for 6 days with the CD40 ligand and IL21. A, Development of plasmablasts was analyzed by using flow cytometry. Numbers indicate percentages of $CD27^+CD38^+$ plasmablasts. B, Immunoglobulin secretion was measured by using ELISA. Data represent means ± SD of triplicates.